

1 Identification and quantification of Lyme pathogen strains by deep 2 sequencing of outer surface protein C (*ospC*) amplicons

3 Lia Di¹, Zhenmao Wan², Saymon Akther², Chunxiao Ying¹, Amanda Larracuente², Li Li², Chong
4 Di¹, Roy Nunez¹, D. Moses Cucura³, Noel L. Goddard^{1,2}, Konstantino Krampis^{1,2,4}, and Wei-Gang
5 Qiu^{1,2,4,#}

6 ¹Department of Biological Sciences, Hunter College of the City University of New York, 695 Park
7 Avenue, New York 10065, USA

8 ²Graduate Center of the City University of New York, 365 Fifth Avenue, New York 10016, USA

9 ³Division of Vector Control, Suffolk County Department of Public Works, Yaphank, New York
10 11980, USA

11 ⁴Department of Physiology and Biophysics & Institute for Computational Biomedicine, Weil
12 Cornell Medical College, New York, New York 10021, USA

13 #Correspondence: Weigang Qiu, weigang@genectr.hunter.cuny.edu

14 Authors' emails & project roles:

- 15 • Lia Di dilie66@gmail.com: Methodology, Investigation, Data Curation, Software, Visualization
- 16 • Zhenmao Wan wanzhenmao@gmail.com: Methodology, Investigation, Writing (original draft)
- 17 • Saymon Akther saymon.akther@gmail.com: Methodology, Investigation, Resources
- 18 • Chunxiao Ying chunxiao.ying@gmail.com: Investigation
- 19 • Amanda Larracuente aslarracuente@gmail.com: Investigation
- 20 • Li Li gift4lily@gmail.com: Resources, Investigation
- 21 • Chong Di chongdi0505@gmail.com: Resources, Visualization
- 22 • Roy Nunez roynunez273@gmail.com: Resources
- 23 • D. Moses Cucura Moses.Cucura@suffolkcountyny.gov: Resources
- 24 • Noel Goddard goddard.noel@gmail.com: Supervision, Funding acquisition
- 25 • Konstantino Krampis agbiotec@gmail.com: Methodology, Funding acquisition, Writing (review &
26 editing)
- 27 • Weigang Qiu weigang@genectr.hunter.cuny.edu: Conceptualization, Funding acquisition,
28 Supervision, Writing (original draft)

29 Short Title: Genotyping Lyme pathogens from ticks

30

31 Abstract

32 Mixed infection of a single tick or host by Lyme disease spirochetes is common and a
33 unique challenge for diagnosis, treatment, and surveillance of Lyme disease. Here we describe a
34 novel protocol for differentiating Lyme strains based on deep sequencing of the hypervariable
35 outer-surface protein C locus (*ospC*). Improving upon the traditional DNA-DNA hybridization
36 method, the next-generation sequencing-based protocol is high-throughput, quantitative, and able
37 to detect new pathogen strains. We applied the method to over one hundred infected *Ixodes*
38 *scapularis* ticks collected from New York State, USA in 2015 and 2016. Analysis of strain
39 distributions within individual ticks suggests an overabundance of multiple infections by five or
40 more strains, inhibitory interactions among co-infecting strains, and presence of a new strain
41 closely related to *Borrelia bissetiae*. A supporting bioinformatics pipeline has been developed.
42 With the newly designed pair of universal *ospC* primers targeting intergenic sequences conserved
43 among all known Lyme pathogens, the protocol could be used for culture-free identification and
44 quantification of Lyme pathogens in wildlife and clinical specimens across the globe.

45
46 Key Words: Lyme disease, *Borrelia*, *Borrelia*, *Ixodes scapularis*, outer surface protein
47 C, next-generation sequencing, frequency-dependent selection

48 Introduction

49 Lyme disease occurs throughout the Northern Hemisphere and is the most prevalent vector-
50 borne diseases in the United States (Hengge et al., 2003; Margos et al., 2011; Schwartz et al.,
51 2017). The causative agents of Lyme disease are obligate bacterial parasites of vertebrates
52 transmitted predominantly by hard-bodied *Ixodes* ticks. Lyme pathogens and related strains,
53 formerly known as the *Borrelia burgdorferi sensu lato* species group, have been recently (and
54 controversially) classified as a new spirochetal genus *Borrelia* (Adeolu and Gupta, 2014;
55 Margos et al., 2017). In the US, while *B. burgdorferi* causes the majority of the Lyme disease
56 cases, more than a half dozen additional *Borrelia* species have been recognized including *B.*
57 *americana*, *B. andersonii*, *B. bissetiae*, *B. californiensis*, *B. carolinensis*, *B. kurtenbachii*, and *B.*
58 *mayonii* (Dolan et al., 2016; Marconi et al., 1995; Margos et al., 2016, 2013; Bobbi S. Pritt et al.,
59 2016; Rudenko et al., 2011, 2009). *Borrelia* species vary not only in genomic sequences but

60 also in geographic distribution, host preferences, human pathogenicity, and disease manifestations
61 (Barbour et al., 2009; Casjens et al., 2018; Kurtenbach et al., 2006; Margos et al., 2011; Mongodin
62 et al., 2013; Bobbi S Pritt et al., 2016). In addition, the *Ixodes* ticks in the US and elsewhere are
63 frequently co-infected with *Borrelia miyamotoii*, a member of the re-defined *Borrelia* genus now
64 consisting exclusively of strains grouped with agents of relapsing fever (Barbour et al., 2009;
65 Wagemakers et al., 2015).

66 A hallmark of Lyme disease endemics is the coexistence of multiple spirochete species and
67 strains within local populations and oftentimes within a single vector, host or patient (Brisson and
68 Dykhuizen, 2004; Durand et al., 2017; Guttman et al., 1996; Qiu, 2008; Seinost et al., 1999; Walter
69 et al., 2016; Wang et al., 1999; Wormser et al., 2008). High genetic diversity within local pathogen
70 populations is to a large extent driven and maintained by frequency-dependent selection under
71 which rare strains gain selective advantage over common ones in establishing super-infection in a
72 host (Bhatia et al., 2018; Durand et al., 2017; Haven et al., 2011; States et al., 2014). In addition,
73 local con-specific strains may have diverged in host specificity and other phenotypes including
74 human virulence and invasiveness (Brisson and Dykhuizen, 2004; Hanincova et al., 2013; Seinost
75 et al., 1999; Wormser et al., 2008). Against this backdrop of the vast geographic, genetic, and
76 phenotypic variations of Lyme disease pathogens across the globe and within endemic regions, it
77 is essential to develop accurate, sensitive, and scalable technologies for identifying species and
78 strains of Lyme pathogens in order to understand, monitor, and control the range expansion of
79 Lyme disease (Kilpatrick et al., 2017; Kurtenbach et al., 2006; Qiu and Martin, 2014).

80 Early molecular technologies for identifying Lyme pathogen strains relied on amplifying
81 and detecting genetic variations at single variable locus including the outer-surface protein A locus
82 (*ospA*), outer surface protein C locus (*ospC*), and the intergenic spacer regions of ribosomal RNA
83 genes (*rrs-rrlA* and *rrfA-rrlB*) (Guttman et al., 1996; Wang et al., 2014, 1999). Availability of the
84 first Lyme pathogen genome facilitated development of more sensitive multilocus sequence typing
85 (MLST) technologies targeting genetic variations at a set of single-copy housekeeping genes
86 (Fraser et al., 1997; Hanincova et al., 2013; Qiu, 2008). For direct identification of Lyme strains
87 in tick and host specimen without first culturing and isolating the organisms, a reverse-line blotting
88 (RLB) technology has been developed based on DNA-DNA hybridization (Brisson and
89 Dykhuizen, 2004; Durand et al., 2015; Morán Cadenas et al., 2007; Qiu et al., 2002). The RLB
90 technology, while sensitive and able to detect mixed infection in tick and hosts, is difficult to scale

91 up or to standardize and does not yield quantitative measures of strain diversity. A further
92 limitation of the RLB technology is that it depends on oligonucleotide probes of known *ospC*
93 major-group alleles and is not able to detect strains with novel *ospC* alleles.

94 Next-generation sequencing (NGS) technologies circumvent the limitations of traditional
95 methods in scalability, standardization, and ability for *de novo* strain detection while offering high
96 sensitivity and high throughput quantification (Lefterova et al., 2015). Using the hybridization
97 capture technology to first enrich pathogen genomes in ticks and subsequently obtaining genome-
98 wide short-read sequences using the Illumina NGS platform, >70% of field-collected nymphal
99 ticks from Northeast and Midwest US are found to be infected with multiple *B. burgdorferi* strains
100 due to mixed inoculum (Walter et al., 2016). In an NGS-based study of European Lyme pathogen
101 populations, a combination of quantitative PCR and high-throughput sequencing on the 454
102 pyrosequencing platform targeting the *ospC* locus and revealed a similarly high rate (77.1%) of
103 mixed infection of nymphal ticks by *B. afzelii* and *B. garinii* (Durand et al., 2017).

104 Here we report an improved NGS technology for identifying Lyme pathogen strains
105 through deep sequencing of *ospC* sequences amplified from individual ticks. We applied the
106 technology to over 100 pathogen-infected *Ixodes scapularis* ticks collected from New York State
107 during a period of two years. Our results suggest a new putative *Borreliella* species, competitive
108 interactions among co-infecting strains, and genetic homogeneity within an endemic region.

109 **Materials & Methods**

110 **Tick collection and DNA extraction**

111 Adult and nymphal blacklegged ticks (*Ixodes scapularis*) were collected in 2015 and 2016
112 during their host-questing seasons from four locations in endemic areas of Lyme disease
113 surrounding New York City (Figure 1). Ticks are stored at -80°C before dissection. Each tick is
114 immersed in 5% solution of Chelex 100 resin (Sigma-Aldrich, St. Louis, MO, USA) containing
115 20mg/ml Proteinase K in milliQ water (EMD Millipore, Billerica, MA, USA) with a total volume
116 of 30µl for nymphs, 100µl for males, and 200µl for females. Ticks are dissected into four or more
117 pieces using sterilized scalpel or disposable pipette tips. The dissected mixture is incubated at 56°C
118 overnight and heated to 100°C for 10 minutes afterwards in a dry bath, and then briefly centrifuged

119 to separate the tick debris and Chelex resin from the supernatant. The supernatant containing the
120 extracted DNA is transferred to a fresh tube and stored at 4°C (or frozen at -20°C for long term
121 storage).

122 **Single-round PCR amplification of full-length *ospC***

123 An improved protocol for amplifying *ospC* sequences from tick DNA extracts has been
124 developed. First, this protocol is simpler with a single instead of two rounds of polymerase-chain
125 reaction (Brisson and Dykhuizen, 2004; Qiu et al., 2002). Second, using a newly designed
126 oligonucleotide primer pair targeting flanking intergenic sequences conserved across *Borrelia*
127 species, we are able to amplify full-length (~718 bp) *ospC* sequences from all strains. Third, the
128 new primers are able to amplify a *vsp* locus in the *B. miyamotoii* genome, enabling co-detection of
129 *Borrelia* species and *Borrelia miyamotoii*, two major groups of Lyme pathogens in Northeast
130 US (Barbour et al., 2009). The new primer sequences are 5'-
131 AATAAAAAGGAGGCACAAATTAATG-3' ("Oc-Fwd", targeting the intergenic spacer
132 between BB_B18 and BB_B19) and 5'-ATATTGACTTTATTTTCCAGTTAC-3' ("Oc-Rev",
133 targeting the intergenic spacer between BB_B19 and BB_B22). Alignments of primer regions for
134 Lyme pathogens are provided as Supplemental Material S1.

135 Each 20µl reaction mixture contains 200 µM of each dNTP, 1U Roche FastStart Taq DNA
136 polymerase (Roche Diagnostics, Mannheim, Germany), 2µl of 10x Roche FastStart Buffer (Roche
137 Diagnostics, California, USA), 0.4µM of each primer and 1µl DNA extract. The reaction mixture
138 is heated at 95°C for 4 minutes, then amplified for 36 cycles at 95°C for 30 seconds, 58°C for 30
139 seconds, and 72°C for 60 seconds, and finally incubated at 72°C for 5 minutes. The PCR products
140 are electrophoresed on a 1% agarose gel, stained with ethidium bromide, and imaged under a UV
141 light. Agencourt AMPure XP PCR Purification Kit (Beckman Coulter, Brea, CA, USA) is used to
142 remove excess primers, dNTPs, and other reagents. Amplicon quantity is measured on the Qubit 4
143 Fluoreometer (Thermo Fisher Scientific, Waltham, MA, USA) using the accompanying Qubit
144 dsDNA HS Assay Kit.

145 **NGS library preparation and short-read sequencing**

146 We followed the Nextera XT DNA Library Prep (Illumina, CA, USA, catalog no. FC-131-
147 1024) protocol to prepare the amplicon libraries for sequencing. First, we dilute the PCR products
148 to 0.2ng/µl after DNA quantification using a DNA 1000 kit on a 2100 BioAnalyzer (Agilent, Santa

149 Clara, CA, USA). Samples are tagmented by incubation of 5µl DNA sample in 55°C for 5 minutes
150 in a solution containing 10µl Tagment DNA Buffer and 5µl Amplicon Tagment Mix.
151 Tagmentation reaction is terminated by adding 5µl Neutralize Tagment Buffer. Tagmented
152 samples are amplified and barcoded (with Set A and Set B) using PCR in a solution containing 5µl
153 of each barcoded primers and the Nextera PCR Mater Mix. The thermal cycling parameters are
154 incubation at 72°C for 3 minutes, 95°C for 30 seconds, 12 cycles of 95°C for 10 seconds, 55°C for
155 30 seconds, and 72°C for 30 seconds, and a final incubation at 72°C for 5 minutes. The indexed
156 amplicon libraries are cleaned using AMPure XP PCR Purification Kit and concentrations
157 quantified using the High-Sensitivity DNA 1000 Kit on a 2100 BioAnalyzer. Amplicon libraries
158 are diluted to the same concentration and then combined to a total concentration of 2 nM to 4 nM
159 with a volume of 5µl or more.

160 In preparation for loading on the MiSeq sequencer, the pooled library is denatured by
161 mixing 5µl of 0.2N NaOH with 5µl of sample and incubating at room temperature for 5 minutes
162 and then adding 990µl pre-chilled Hybridization Buffer, resulting in a total of 1 ml (10pM
163 concentration) of denatured pooled amplicon library (Illumina Denature and Dilute Libraries
164 Guide pub. no. 15039740). Furthermore, 5% PhiX Sequencing Control (Illumina, CA, USA,
165 catalog no. FC-110-3001) is added to the samples pool before loading to the MiSeq. The
166 sequencing kit used is the MiSeq Reagent Kit v3 for 150 cycles (Illumina, CA, USA, catalog no.
167 MS-102-3001), for paired reads of 75 bases each. Following sequencing, a total of 4.24 gigabases
168 of sequence are generated by the instrument, corresponding to 57,463,220 reads, with
169 approximately 90% of the reads (52,311,968) passing the filter build-in the MiSeq for quality
170 control. Finally, the samples are automatically de-multiplexed to individual FASTQ files following
171 completion of the sequencing run by the MiSeq Reporter Software based on the Nextera XT
172 barcodes corresponding to each sample (the barcodes are also trimmed by the software from each
173 read).

174 **Amplicon cloning & Sanger sequencing**

175 New alleles are identified when the majority of reads are not aligned to reference
176 sequences. For such samples, we performed *de novo* assembly of short reads to obtain candidate
177 allele sequences (see below). The novel alleles are subsequently validated by cloning and Sanger
178 sequencing. Cloning of PCR products is performed using the TOPO TA Cloning Kit for

179 Sequencing (Thermo Fisher Scientific, Waltham, MA, USA) following manufacturer's protocol.
180 Five bacterial colonies containing plasmids with PCR amplicon as inserts are selected for further
181 growth in selective liquid media. Plasmid DNA is extracted and purified using the PureLink Quick
182 Plasmid Miniprep Kits (Thermo Fisher Scientific, Waltham, MA, USA). Nucleotide sequences of
183 cloned PCR amplicons are obtained using the Sanger method through commercial sequencing services
184 including Genewiz (South Plainfield, NJ, USA) and Macrogen (Rockville, MD, USA).

185 **Bioinformatics methods for allele identification and quantification**

186 Alleles present in tick samples are identified and quantified by aligning the paired-end
187 short reads to a set of reference sequences. These reference sequences consist of full-length *ospC*
188 sequences and are obtained from published genome sequences, from Sanger sequencing of cloned
189 or uncloned amplicons (see above), or from *de novo* assembly of short reads (see below) (the 20
190 reference sequences are listed in Supplemental Material S2).

191 The short reads are indexed and aligned to the reference sequences using software packages
192 bwa (Li and Durbin, 2009) and samtools (Li et al., 2009). Coverage of reads at each site of each
193 reference sequence is obtained by using bedtools (Quinlan and Hall, 2010) and visualized using
194 ggplot2 in the R statistical computing environment (R Core Team, 2013; Wickham, 2009).
195 Presence of new alleles is noted when a large number of reads are unmapped. For these samples,
196 we cloned the PCR amplicons and sequenced the clones using Sanger sequencing (see above). A
197 number of known alleles do not have full-length *ospC* sequences from sequenced genomes or from
198 GenBank. For these alleles, we performed *de novo* assembly of reads to obtain the 5'- and 3'-end
199 sequences using the assembler metaSPAdes (Nurk et al., 2017).

200 To test the accuracy and sensitivity of our bioinformatics pipelines, we generated simulated
201 short reads with known allele identities and known proportions of allele mixture using wgsim, a
202 part of the software samtools package (Li et al., 2009). Key steps and commands for allele
203 identification, coverage calculation, *de novo* assembly, and simulated reads are provided as
204 Supplemental Material S3.

205 **Statistical analysis of genetic diversity**

206 We estimate the relative amount of spirochete load in individual infected ticks by the
207 weight (in ng) of PCR amplicons. Diversity of *ospC* alleles in individual infected ticks is first

208 measured with multiplicity, i.e., the number of unique alleles present in a sample. Allelic diversity
209 is further measured with the Shannon diversity index $\alpha = 1 - \frac{-\sum p_i \log(p_i)}{\log(n)}$, where p_i is the
210 frequency of allele i and n is the number of distinct alleles in an infected tick (allowing $\alpha=0$ for
211 $n=1$). This Shannon diversity index, also known as the Shannon Equitability Index, is a normalized
212 measure of biodiversity ranging from 0 (infected with a single strain) to 1 (all strains being equally
213 frequent) (Vidakovic, 2011). Allele frequencies in an infected tick are obtained as $p_i =$
214 $C_i / \sum_{j=1}^n C_j$, where C_i is the coverage of allele i averaged over all nucleotide positions.

215 Genetic differentiation between two populations (A and B) is measured with the F_{st}
216 statistics: $F_{st} = \frac{H_T - [n_A H_S(A) + n_B H_S(B)]}{(n_A + n_B) H_T}$ (Nei, 1973), where $H_S(A)$, $H_S(B)$, and H_T are heterozygosity
217 of sample A, sample B, and the total sample, respectively, and n_A and n_B are the sample sizes.
218 Statistical significance of an F_{st} value is estimated by a randomization procedure by which the two
219 population samples are combined and randomly divided into two pseudo-samples with the same
220 sample sizes. An F_{st} value is calculated between the two pseudo-samples. The procedure is
221 repeated for 999 times and a p -value is obtain as the proportion of permuted F_{st} values that is
222 greater than or equal to the observed value. Genetic differentiation is further tested using F -
223 statistics implemented in the *hierfstat* package on the R statistical computing environment
224 (Goudet, 2005).

225 Data availability

226 New sequences have been deposited in GenBank with consecutive accessions MH071430
227 through MH071436. Experimental data are stored in a custom relational database. An interactive
228 website has been developed using the D3js (<http://d3js.org>) JavaScript library to visualize allele
229 composition and read depth for the 119 tick samples and is publicly available at
230 <http://diverge.hunter.cuny.edu/~weigang/ospC-sequencing/>. Data sets and R scripts are publicly
231 available at Github <https://github.com/weigangq/ocseq>.

232 Results

233 Tick infection rates, co-infections, specificity, and sensitivity

234 Approximately 25% of nymphal ticks and 50% of adult ticks are infected with *Borrelia*

235 species or *Borrelia miyamotoi*. For example, the nymphal infection rate for *Borrelia burgdorferi*
236 is 27.9% (with a 95% confidence interval of 15.3 – 43.7%) in Sample #7 and the adult infection
237 rate for *Borrelia burgdorferi* is 42.1% (32.9 – 51.7%) for Sample #9 (Figure 1). The infection
238 rate for *Borrelia miyamotoi* in adult ticks is 6.1% (7 out of 114 ticks; 2.5 – 12.2% confidence
239 interval) for Sample #9. Four ticks in Sample #9 are infected with both *Borrelia burgdorferi*
240 and *Borrelia miyamotoi* (co-infection rate 3.5%, 0.96-8.74%). Rates from other samples are
241 underestimates due to lack of success in tick storage, processing, DNA amplification, and NGS
242 sequencing during protocol development. These rates are consistent with results from other studies
243 conducted in the same region and appear to be stable through recent decades (Qiu et al., 2002;
244 States et al., 2014).

245 The number of sequencing averages ~108,000 reads per tick sample. The coverage (i.e.,
246 read depth) of an allele depends on the total number of tick samples in a pooled library and the
247 number of alleles present in a tick. Alleles are identified if the reads cover all nucleotide positions
248 of a reference allele and the total read percentage is at least 1% of the most abundant alleles. The
249 total sample of 119 successfully sequenced ticks are divided into four sub-population samples
250 according to geographic origin and life stage, with allele counts of pathogens in each of the four
251 populations listed in Table 1.

252 Specificity of allele identification is tested by generating simulated reads from a single
253 reference sequence and aligning the simulated reads to all reference sequences. This simulation-
254 based test shows that the bioinformatics protocol for allele identification is highly specific, with
255 only a small fraction of ambiguously aligned reads at the first ~200 conserved positions for some
256 *ospC* alleles (Supplemental Material S4).

257 Sensitivity of allele quantification is tested by generating a known proportion of simulated
258 reads from two reference sequences. For example, a 10:1 mixed sample of short reads generated
259 based on sequences of alleles “J” and “C” is quantified using the bioinformatics protocol, resulting
260 in a ~13:1 quantification (Figure 2A).

261 **New strain, spirochete load, and multiplicity**

262 The NGS protocol is able to not only detect the presence of multiple strains but also
263 quantify their relative frequency in individual ticks infected by multiple strains (Figure 2B). One
264 allele (labeled as “C14_N150”) does not have known high-identity homologs in GenBank, with

265 the top BLASTp hit as the *B. bissetiae* strain 25015 *ospC* with 75% identity in protein sequence
266 (ACC45540) (Tilly et al., 1997). This allele likely represents an un-identified *Borrelia* species
267 (Figure 2C). This allele was cloned, sequenced with Sanger method, and assigned a GenBank
268 accession (MH071431). The full-length “F” allele was similarly cloned, sequenced with Sanger
269 method, and assigned a GenBank accession (MH071432). The full-length “O” allele (MH071435)
270 was sequenced with Sanger method directly from the singly-infected tick #N045 without cloning
271 of the PCR amplicon. Sequences of full-length alleles “B3”, “N”, and “T” (MH071430,
272 MH071433, and MH071436) were obtained by *de novo* assembly of short reads using metaSPAdes
273 (Nurk et al., 2017). Our protocol is able to detect infection by *Borrelia miyamotoii*, as shown by
274 the presence of one of its *vsp* (variable surface protein gene, locus name AXH25_04790)
275 amplicons in samples (Figure 2D). The *vsp* allele was cloned, sequenced with Sanger method, and
276 assigned a GenBank accession (MH071435).

277 Assuming that the spirochete load is correlated with total weight of PCR amplicons, we
278 found that female adult ticks carry a significantly higher spirochete load than male adult ticks
279 ($p=0.022$ by *t*-test), which in turn carry a higher infection load than nymphal ticks ($p=8.1e-3$)
280 (Figure 3A). There is no significant difference in the average number of strains infecting a single
281 tick ($p>0.5$ by Mann-Whitney test), although the median values are two strains per infected adult
282 tick and one strain per nymphal tick (Figure 3B). Similarly, there are no significant differences in
283 strain diversity measured by the Shannon diversity index between male, female, and nymphal ticks
284 ($p>0.5$ by Mann-Whitney test; Figure 3C).

285 **Aggregated infection & negative strain interactions**

286 A previous study of multi-strain infection by *B. afzelii* in Europe found that strains tend to
287 be aggregated in infected ticks, suggesting that infection of ticks and hosts is more successfully
288 established by multiple spirochete strains than by a single strain alone (Andersson et al., 2013).
289 Our data support their conclusion. In Sample #9, for example, we detected a total of 159 *ospC*
290 alleles in 55 infected ticks out of a total of 114 processed adult ticks. Assuming a Poisson model
291 of independent infection of individual strains with an average successful infection rate
292 $\lambda=159/114=1.395$ strains per tick, we expect on average 28.2 uninfected ticks and 39.4 ticks
293 infected by a single strain (the observed and expected counts are plotted in Figure 3D). In fact, 59
294 ticks are uninfected in this sample, more than twice the expected count. Meanwhile, 22 ticks are

295 infected by a single strain, approximately half of the expected number. It appears that ticks tend to
296 be either free of infection or infected by multiple spirochete strains, supporting the aggregated
297 infection hypothesis (Andersson et al., 2013).

298 In infected ticks, previous studies conclude either a negative or a lack of interactions among
299 co-infecting strains (Andersson et al., 2013; Durand et al., 2017; Walter et al., 2016). Our analysis
300 supports presence of negative or inhibitory interactions among co-infecting strains. First, multiple
301 strains tend to be unevenly distributed in their spirochete loads with some strains dominating others
302 (e.g., Figure 2B). This is more generally shown with the Shannon diversity index, which is on
303 average approximately half of the maximum attainable diversity (when all strains are equally
304 abundant) in ticks with mixed infections (Supplemental Figure S5). There is, however, no evidence
305 that any particular strains are consistently more dominant than other (Supplemental Figure S5).
306 Second, when strains are independent from each other or facilitating each other's growth, one
307 expects ticks infected with multiple strains to have a higher spirochete load than ticks infected with
308 a single strain. Conversely, if strains inhibit each other within a host or vector, one expects the
309 total spirochete load to be either lower in ticks infected by multiple than by single strains or at
310 similar levels. We plot the total pathogen load with respect to multiplicity or the Shannon diversity
311 index in individual ticks (Figure 4). For the most part, the regression lines are not significantly
312 different from a slope of zero except that the spirochete load in nymphs decreases significantly
313 with increasing number of strains. The overall flat trend supports negative rather than facilitating
314 interactions or a lack of any interactions between co-infecting strains (Durand et al., 2017; Walter
315 et al., 2016).

316 **Similar strain distributions among regions and life stages**

317 Spirochete populations infecting adult and nymph ticks are similar in strain composition
318 ($F_{ST}=4.7e-3$ and $p=0.089$ by resampling, $p=0.369$ by F -test) (Figures 5A & 5C). Genetic
319 differentiation between the Upper State and Long Island populations is more pronounced but
320 nonetheless lacks statistical significance ($F_{ST}=5.3e-3$ and $p=0.052$ by resampling, $p=0.245$ by F -
321 test). The groups F and J strains appear to be more common on Long Island than Upper State
322 while the group L strain shows the opposite pattern of distribution (Figures 5B & D).

323 Discussion

324 In this report, we describe a new experimental and bioinformatics protocol for detecting
325 and quantifying Lyme disease pathogen strains infecting individual ticks based on next-generation
326 sequencing technology. Improving upon the previous Reverse-Line Blotting technology, the
327 protocol allows *de novo* detection of previously unknown pathogen strains. Indeed, one of the ticks
328 carries a putative new *Borrelia* species with a novel *ospC* allele (“C14”, MH071431). The
329 protocol is highly sensitive and specific, enabling quantification of genetic diversity within single
330 ticks and rigorously testing ecological hypotheses such as strain interactions (Figures 4) and
331 genetic differentiation (Figure 5).

332 High-throughput sequencing has previously been used for quantification of Lyme strains
333 in ticks based on either genome capture or *ospC* amplicons (Durand et al., 2017; Walter et al.,
334 2016). Our technology is novel for an improved PCR protocol by using a set of universal PCR
335 primers able to amplify full-length *ospC* in all *Borrelia* species as well as the *vsp* locus in
336 *Borrelia miyamotoi*. Further, the PCR protocol is simplified from two rounds to a single round of
337 thermal cycling. Due to these critical improvements in PCR protocol, our method could be readily
338 used for detection and quantification of a broad range of Lyme disease (and possibly relapsing
339 fever) pathogens in clinical and wildlife specimens across their species ranges worldwide. In
340 addition, our technology is novel in using the Illumina short-read sequencing platform, in its
341 supporting bioinformatics pipelines, and in its application to *Ixodes* ticks in North America.

342 Our strain identification method is based on the assumption of a strict one-to-one
343 correspondence (i.e., complete genetic linkage) between *ospC* alleles and *B. burgdorferi* strains.
344 The *ospC* locus is the most polymorphic single-copy locus in the *Borrelia* genome (Mongodin
345 et al., 2013). The linkage between the *ospC* locus and the whole genome is indeed nearly complete
346 for *Borrelia* populations in Northeast United States (Casjens et al., 2017; Mongodin et al., 2013).
347 In fact, diversification of strains in local *Borrelia* populations is likely driven by frequency-
348 dependent selection targeting the *ospC* locus (Haven et al., 2011; Qiu and Martin, 2014). However,
349 linkage between *ospC* and other genomic loci is weaker in Midwestern and Southern US
350 populations due to recombination and plasmid exchange (Hanincova et al., 2013; Mechai et al.,
351 2015). Cross-species and cross-strain exchange of *ospC* alleles is also common in European
352 populations. For example, whole genome sequencing showed that the European *B. burgdorferi*

353 strain BOL26 obtained its *ospC* and its flanking genes from a con-specific strain through horizontal
354 gene transfer (Qiu and Martin, 2014). For population samples elsewhere, therefore, it might be
355 necessary to add a 2nd locus for strain identification (Barbour and Cook, 2018). One complemental
356 genetic marker could be the rRNA spacer (*rrs-rrlA*), which is a single-copy and highly variable
357 locus (Wang et al., 2014). Experimental methods for high-throughput sequencing of the *rrs-rrlA*
358 locus however are yet to be developed.

359 While we are able to estimate relative spirochete loads in individual ticks based on
360 quantification of *ospC* amplicons (Figure 2A), we have not attempted to directly quantify the
361 number of spirochetes in infected ticks using methods such as quantitative PCR (Durand et al.,
362 2017). In the future, we plan to quantify spirochete loads in individual ticks by running our
363 experimental and bioinformatics procedures with known quantities of genomic DNA and
364 generating a standard calibration curve.

365 Nonetheless, using relative estimates of spirochete loads in individual ticks, we are able to
366 validate a number of hypotheses on multi-strain infections. First, the lack of differences in strain
367 diversity between the questing adult ticks, which have taken two blood meals, and the questing
368 nymphal ticks, which have taken one blood meal (Figure 3), supports the conclusion that strain
369 diversity in individual ticks is for the most part due to mixed inoculum in infected hosts (Walter
370 et al., 2016). Second, ticks are more likely to be infected by five or more strains than expected by
371 chance (Figure 4D), supporting the aggregated infection hypothesis (Andersson et al., 2013).
372 Rather than strains actively facilitating each other in establishing infections, however, strain
373 aggregation in ticks may be a reflection of reservoir hosts being either free of spirochetes (in the
374 case of resistant and healthy hosts) or infected by multiple strains (in the case of susceptible and
375 weakened hosts). Regardless, it appears that once a host is infected by a strain, it becomes
376 susceptible for super-infection by additional, immunologically distinct strains (Bhatia et al., 2018).
377 Third, we found an uneven distribution of strains in infected ticks as well as a flat or decreasing
378 spirochete load with increasing strain diversity (Figure 5), supporting inhibitory interactions
379 among co-infecting strains driven by competitive growth in reservoir hosts (Durand et al., 2017;
380 Walter et al., 2016). Fourth, we found weak genetic differentiation between populations from the
381 two New York City suburbs (Figure 5B), suggesting either a recent common origin, or similar
382 reservoir hosts, or both. Fifth, we observed co-circulation of *B. miyamotoii* and other *Borrelia*
383 species in the same area. The lower prevalence as well as lower genetic diversity at *ospC* or *vsp*

384 loci of these low-prevalence spirochetes relative to those of *B. burgdorferi* suggests that *ospC*
385 hypervariability may be a key adaptation underlining the ecological success of *B. burgdorferi* in
386 this region.

387 To summarize, we have established a next-generation sequencing-based, taxonomically
388 broad procedure that has the potential to become a standard protocol for detecting and quantifying
389 Lyme disease pathogens across the globe. The increased sensitivity of high-throughput sequencing
390 technologies employed here and elsewhere highlights the prevalence of multiple infections in
391 wildlife samples and a pressing need for broad spectrum vaccines for control and prevention of
392 Lyme disease (Earnhart et al., 2007; Livey et al., 2011).

393 Acknowledgements

394 We thank Ms Li Zhai and Dr Edward Skolnik of New York University School of Medicine
395 for facilitating cloning experiments and Mr Brian Sulkow for participation of fieldwork. This work
396 was supported by Public Health Service grants AI107955 (to WGQ) from the National Institute of
397 Allergy and Infectious Diseases (NIAID) and the grant MD007599 (to Hunter College) from the
398 National Institute on Minority Health and Health Disparities (NIMHD) of the National Institutes
399 of Health (NIH) of the United States of America. The content of this manuscript is solely the
400 responsibility of the authors and do not necessarily represent the official views of NIAID, NIMHD,
401 or NIH.

402 References

- 403 Adeolu, M., Gupta, R.S., 2014. A phylogenomic and molecular marker based proposal for the division of
404 the genus *Borrelia* into two genera: the emended genus *Borrelia* containing only the members
405 of the relapsing fever *Borrelia*, and the genus *Borrelia* gen. nov. containing the members of
406 the Lyme disease *Borrelia* (*Borrelia burgdorferi* sensu lato complex). *Antonie Van Leeuwenhoek*
407 105, 1049–1072. <https://doi.org/10.1007/s10482-014-0164-x>
- 408 Andersson, M., Scherman, K., Råberg, L., 2013. Multiple-strain infections of *Borrelia afzelii*: a role for
409 within-host interactions in the maintenance of antigenic diversity? *Am. Nat.* 181, 545–554.
410 <https://doi.org/10.1086/669905>
- 411 Barbour, A.G., Bunikis, J., Travinsky, B., Hoen, A.G., Diuk-Wasser, M.A., Fish, D., Tsao, J.I., 2009. Niche
412 partitioning of *Borrelia burgdorferi* and *Borrelia miyamotoi* in the same tick vector and
413 mammalian reservoir species. *Am. J. Trop. Med. Hyg.* 81, 1120–1131.
414 <https://doi.org/10.4269/ajtmh.2009.09-0208>
- 415 Barbour, A.G., Cook, V.J., 2018. Genotyping Strains of Lyme Disease Agents Directly From Ticks, Blood,

- 416 or Tissue, in: *Borrelia burgdorferi*, Methods in Molecular Biology. Humana Press, New York, NY,
417 pp. 1–11. https://doi.org/10.1007/978-1-4939-7383-5_1
- 418 Bhatia, B., Hillman, C., Carracoi, V., Cheff, B.N., Tilly, K., Rosa, P.A., 2018. Infection history of the
419 blood-meal host dictates pathogenic potential of the Lyme disease spirochete within the
420 feeding tick vector. *PLOS Pathog.* 14, e1006959. <https://doi.org/10.1371/journal.ppat.1006959>
- 421 Brisson, D., Dykhuizen, D.E., 2004. ospC Diversity in *Borrelia burgdorferi* Different Hosts Are Different
422 Niches. *Genetics* 168, 713–722. <https://doi.org/10.1534/genetics.104.028738>
- 423 Casjens, S.R., Di, L., Akther, S., Mongodin, E.F., Luft, B.J., Schutzer, S.E., Fraser, C.M., Qiu, W.-G.,
424 2018. Primordial origin and diversification of plasmids in Lyme disease agent bacteria. *BMC*
425 *Genomics* 19, 218. <https://doi.org/10.1186/s12864-018-4597-x>
- 426 Casjens, S.R., Gilcrease, E.B., Vujadinovic, M., Mongodin, E.F., Luft, B.J., Schutzer, S.E., Fraser, C.M.,
427 Qiu, W.-G., 2017. Plasmid diversity and phylogenetic consistency in the Lyme disease agent
428 *Borrelia burgdorferi*. *BMC Genomics* 18, 165. <https://doi.org/10.1186/s12864-017-3553-5>
- 429 Dolan, M.C., Hojgaard, A., Hoxmeier, J.C., Replogle, A.J., Respicio-Kingry, L.B., Sexton, C., Williams,
430 M.A., Pritt, B.S., Schriefer, M.E., Eisen, L., 2016. Vector competence of the blacklegged tick,
431 *Ixodes scapularis*, for the recently recognized Lyme borreliosis spirochete *Candidatus Borrelia*
432 *mayonii*. *Ticks Tick-Borne Dis.* <https://doi.org/10.1016/j.ttbdis.2016.02.012>
- 433 Durand, J., Herrmann, C., Genné, D., Sarr, A., Gern, L., Voordouw, M.J., 2017. Multistrain Infections
434 with Lyme Borreliosis Pathogens in the Tick Vector. *Appl. Environ. Microbiol.* 83, e02552-16.
435 <https://doi.org/10.1128/AEM.02552-16>
- 436 Durand, J., Jacquet, M., Paillard, L., Rais, O., Gern, L., Voordouw, M.J., 2015. Cross-Immunity and
437 Community Structure of a Multiple-Strain Pathogen in the Tick Vector. *Appl. Environ.*
438 *Microbiol.* 81, 7740–7752. <https://doi.org/10.1128/AEM.02296-15>
- 439 Earnhart, C.G., Buckles, E.L., Marconi, R.T., 2007. Development of an OspC-based tetravalent,
440 recombinant, chimeric vaccinogen that elicits bactericidal antibody against diverse Lyme
441 disease spirochete strains. *Vaccine* 25, 466–480. <https://doi.org/10.1016/j.vaccine.2006.07.052>
- 442 Fraser, C.M., Casjens, S., Huang, W.M., Sutton, G.G., Clayton, R., Lathigra, R., White, O., Ketchum,
443 K.A., Dodson, R., Hickey, E.K., Gwinn, M., Dougherty, B., Tomb, J.-F., Fleischmann, R.D.,
444 Richardson, D., Peterson, J., Kerlavage, A.R., Quackenbush, J., Salzberg, S., Hanson, M., Vugt,
445 R. van, Palmer, N., Adams, M.D., Gocayne, J., Weidman, J., Utterback, T., Watthey, L.,
446 McDonald, L., Artiach, P., Bowman, C., Garland, S., Fujii, C., Cotton, M.D., Horst, K., Roberts,
447 K., Hatch, B., Smith, H.O., Venter, J.C., 1997. Genomic sequence of a Lyme disease spirochaete,
448 *Borrelia burgdorferi*. *Nature* 390, 580–586. <https://doi.org/10.1038/37551>
- 449 Goudet, J., 2005. hierfstat, a package for r to compute and test hierarchical F-statistics. *Mol. Ecol.*
450 *Notes* 5, 184–186. <https://doi.org/10.1111/j.1471-8286.2004.00828.x>
- 451 Guttman, D.S., Wang, P.W., Wang, I.N., Bosler, E.M., Luft, B.J., Dykhuizen, D.E., 1996. Multiple
452 infections of *Ixodes scapularis* ticks by *Borrelia burgdorferi* as revealed by single-strand
453 conformation polymorphism analysis. *J. Clin. Microbiol.* 34, 652–656.
- 454 Hanincova, K., Mukherjee, P., Ogden, N.H., Margos, G., Wormser, G.P., Reed, K.D., Meece, J.K.,
455 Vandermause, M.F., Schwartz, I., 2013. Multilocus Sequence Typing of *Borrelia burgdorferi*
456 Suggests Existence of Lineages with Differential Pathogenic Properties in Humans. *PLoS ONE*
457 8, e73066. <https://doi.org/10.1371/journal.pone.0073066>
- 458 Haven, J., Vargas, L.C., Mongodin, E.F., Xue, V., Hernandez, Y., Pagan, P., Fraser-Liggett, C.M.,
459 Schutzer, S.E., Luft, B.J., Casjens, S.R., Qiu, W.-G., 2011. Pervasive Recombination and
460 Sympatric Genome Diversification Driven by Frequency-Dependent Selection in *Borrelia*
461 *burgdorferi*, the Lyme Disease Bacterium. *Genetics* 189, 951–966.
462 <https://doi.org/10.1534/genetics.111.130773>
- 463 Hengge, U.R., Tannapfel, A., Tying, S.K., Erbel, R., Arendt, G., Ruzicka, T., 2003. Lyme borreliosis.

- 464 Lancet Infect. Dis. 3, 489–500.
- 465 Kilpatrick, A.M., Dobson, A.D.M., Levi, T., Salkeld, D.J., Swei, A., Ginsberg, H.S., Kjemtrup, A., Padgett,
466 K.A., Jensen, P.M., Fish, D., Ogden, N.H., Diuk-Wasser, M.A., 2017. Lyme disease ecology in a
467 changing world: consensus, uncertainty and critical gaps for improving control. *Philos. Trans. R.*
468 *Soc. Lond. B. Biol. Sci.* 372. <https://doi.org/10.1098/rstb.2016.0117>
- 469 Kurtenbach, K., Hanincová, K., Tsao, J.I., Margos, G., Fish, D., Ogden, N.H., 2006. Fundamental
470 processes in the evolutionary ecology of Lyme borreliosis. *Nat. Rev. Microbiol.* 4, 660–669.
471 <https://doi.org/10.1038/nrmicro1475>
- 472 Lefterova, M.I., Suarez, C.J., Banaei, N., Pinsky, B.A., 2015. Next-Generation Sequencing for Infectious
473 Disease Diagnosis and Management. *J. Mol. Diagn.* 17, 623–634.
474 <https://doi.org/10.1016/j.jmoldx.2015.07.004>
- 475 Li, H., Handsaker, B., Wysoker, A., Fennell, T., Ruan, J., Homer, N., Marth, G., Abecasis, G., Durbin, R.,
476 1000 Genome Project Data Processing Subgroup, 2009. The Sequence Alignment/Map format
477 and SAMtools. *Bioinforma. Oxf. Engl.* 25, 2078–2079.
478 <https://doi.org/10.1093/bioinformatics/btp352>
- 479 Livey, I., O'Rourke, M., Traweger, A., Savidis-Dacho, H., Crowe, B.A., Barrett, P.N., Yang, X., Dunn, J.J.,
480 Luft, B.J., 2011. A new approach to a Lyme disease vaccine. *Clin. Infect. Dis. Off. Publ. Infect.*
481 *Dis. Soc. Am.* 52 Suppl 3, s266-270. <https://doi.org/10.1093/cid/ciq118>
- 482 Marconi, R.T., Liveris, D., Schwartz, I., 1995. Identification of novel insertion elements, restriction
483 fragment length polymorphism patterns, and discontinuous 23S rRNA in Lyme disease
484 spirochetes: phylogenetic analyses of rRNA genes and their intergenic spacers in *Borrelia*
485 *japonica* sp. nov. and genomic group 21038 (*Borrelia andersonii* sp. nov.) isolates. *J. Clin.*
486 *Microbiol.* 33, 2427–2434.
- 487 Margos, G., Lane, R.S., Fedorova, N., Koloczek, J., Piesman, J., Hojgaard, A., Sing, A., Fingerle, V.,
488 2016. *Borrelia bissettae* sp. nov. and *Borrelia californiensis* sp. nov. prevail in diverse enzootic
489 transmission cycles. *Int. J. Syst. Evol. Microbiol.* 66, 1447–1452.
490 <https://doi.org/10.1099/ijsem.o.000897>
- 491 Margos, G., Marosevic, D., Cutler, S., Derdakova, M., Diuk-Wasser, M., Emler, S., Fish, D., Gray, J.,
492 Hunfeldt, K.-P., Jaulhac, B., Kahl, O., Kovalev, S., Kraiczy, P., Lane, R.S., Lienhard, R., Lindgren,
493 P.E., Ogden, N., Ornstein, K., Rupprecht, T., Schwartz, I., Sing, A., Straubinger, R.K., Strle, F.,
494 Voordouw, M., Rizzoli, A., Stevenson, B., Fingerle, V., 2017. There is inadequate evidence to
495 support the division of the genus *Borrelia*. *Int. J. Syst. Evol. Microbiol.* 67, 1081–1084.
496 <https://doi.org/10.1099/ijsem.o.001717>
- 497 Margos, G., Piesman, J., Lane, R.S., Ogden, N.H., Sing, A., Straubinger, R.K., Fingerle, V., 2013. *Borrelia*
498 *kurtenbachii* sp. nov.: A widely distributed member of the *Borrelia burgdorferi* sensu lato
499 species complex in North America. *Int. J. Syst. Evol. Microbiol.*
500 <https://doi.org/10.1099/ijs.o.054593-0>
- 501 Margos, G., Vollmer, S.A., Ogden, N.H., Fish, D., 2011. Population genetics, taxonomy, phylogeny and
502 evolution of *Borrelia burgdorferi* sensu lato. *Infect. Genet. Evol.* 11, 1545–1563.
503 <https://doi.org/10.1016/j.meegid.2011.07.022>
- 504 Mechai, S., Margos, G., Feil, E.J., Lindsay, L.R., Ogden, N.H., 2015. Complex population structure of
505 *Borrelia burgdorferi* in southeastern and south central Canada as revealed by phylogeographic
506 analysis. *Appl. Environ. Microbiol.* 81, 1309–1318. <https://doi.org/10.1128/AEM.03730-14>
- 507 Mongodin, E.F., Casjens, S.R., Bruno, J.F., Xu, Y., Drabek, E.F., Riley, D.R., Cantarel, B.L., Pagan, P.E.,
508 Hernandez, Y.A., Vargas, L.C., Dunn, J.J., Schutzer, S.E., Fraser, C.M., Qiu, W.-G., Luft, B.J.,
509 2013. Inter- and intra-specific pan-genomes of *Borrelia burgdorferi* sensu lato: genome stability
510 and adaptive radiation. *BMC Genomics* 14, 693. <https://doi.org/10.1186/1471-2164-14-693>
- 511 Morán Cadenas, F., Rais, O., Humair, P.-F., Douet, V., Moret, J., Gern, L., 2007. Identification of host

- 512 bloodmeal source and *Borrelia burgdorferi* sensu lato in field-collected *Ixodes ricinus* ticks in
513 Chaumont (Switzerland). *J. Med. Entomol.* 44, 1109–1117.
- 514 Nei, M., 1973. Analysis of gene diversity in subdivided populations. *Proc. Natl. Acad. Sci. U. S. A.* 70,
515 3321–3323.
- 516 Nurk, S., Meleshko, D., Korobeynikov, A., Pevzner, P.A., 2017. metaSPAdes: a new versatile
517 metagenomic assembler. *Genome Res.* 27, 824–834. <https://doi.org/10.1101/gr.213959.116>
- 518 Pritt, Bobbi S, Mead, P.S., Johnson, D.K.H., Neitzel, D.F., Respicio-Kingry, L.B., Davis, J.P., Schiffman,
519 E., Sloan, L.M., Schriefer, M.E., Replogle, A.J., Paskewitz, S.M., Ray, J.A., Bjork, J., Steward,
520 C.R., Deedon, A., Lee, X., Kingry, L.C., Miller, T.K., Feist, M.A., Theel, E.S., Patel, R., Irish, C.L.,
521 Petersen, J.M., 2016. Identification of a novel pathogenic *Borrelia* species causing Lyme
522 borreliosis with unusually high spirochaetaemia: a descriptive study. *Lancet Infect. Dis.*
523 [https://doi.org/10.1016/S1473-3099\(15\)00464-8](https://doi.org/10.1016/S1473-3099(15)00464-8)
- 524 Pritt, Bobbi S., Respicio-Kingry, L.B., Sloan, L.M., Schriefer, M.E., Replogle, A.J., Bjork, J., Liu, G.,
525 Kingry, L.C., Mead, P.S., Neitzel, D.F., Schiffman, E., Hoang Johnson, D.K., Davis, J.P.,
526 Paskewitz, S.M., Boxrud, D., Deedon, A., Lee, X., Miller, T.K., Feist, M.A., Steward, C.R., Theel,
527 E.S., Patel, R., Irish, C.L., Petersen, J.M., 2016. *Borrelia mayonii* sp. nov., a member of the
528 *Borrelia burgdorferi* sensu lato complex, detected in patients and ticks in the upper midwestern
529 United States. *Int. J. Syst. Evol. Microbiol.* 66, 4878–4880.
530 <https://doi.org/10.1099/ijsem.0.001445>
- 531 Qiu, W.-G., 2008. Wide Distribution of a High-Virulence *Borrelia burgdorferi* Clone in Europe and North
532 America. *Emerg. Infect. Dis.* 14, 1097–1104. <https://doi.org/10.3201/eid1407.070880>
- 533 Qiu, W.-G., Dykhuizen, D.E., Acosta, M.S., Luft, B.J., 2002. Geographic Uniformity of the Lyme Disease
534 Spirochete (*Borrelia burgdorferi*) and Its Shared History With Tick Vector (*Ixodes scapularis*) in
535 the Northeastern United States. *Genetics* 160, 833–849.
- 536 Qiu, W.-G., Martin, C.L., 2014. Evolutionary genomics of *Borrelia burgdorferi* sensu lato: Findings,
537 hypotheses, and the rise of hybrids. *Infect. Genet. Evol.* 27C, 576–593.
538 <https://doi.org/10.1016/j.meegid.2014.03.025>
- 539 Quinlan, A.R., Hall, I.M., 2010. BEDTools: a flexible suite of utilities for comparing genomic features.
540 *Bioinforma. Oxf. Engl.* 26, 841–842. <https://doi.org/10.1093/bioinformatics/btq033>
- 541 R Core Team, 2013. R: A Language and Environment for Statistical Computing. R Foundation for
542 Statistical Computing.
- 543 Rudenko, N., Golovchenko, M., Grubhoffer, L., Oliver, J.H., 2011. *Borrelia carolinensis* sp. nov., a novel
544 species of the *Borrelia burgdorferi* sensu lato complex isolated from rodents and a tick from the
545 south-eastern USA. *Int. J. Syst. Evol. Microbiol.* 61, 381–383.
546 <https://doi.org/10.1099/ijms.0.021436-0>
- 547 Rudenko, N., Golovchenko, M., Lin, T., Gao, L., Grubhoffer, L., Oliver, J.H., Jr, 2009. Delineation of a
548 new species of the *Borrelia burgdorferi* Sensu Lato Complex, *Borrelia americana* sp. nov. *J. Clin.*
549 *Microbiol.* 47, 3875–3880. <https://doi.org/10.1128/JCM.01050-09>
- 550 Schwartz, A.M., Hinckley, A.F., Mead, P.S., Hook, S.A., Kugeler, K.J., 2017. Surveillance for Lyme
551 Disease - United States, 2008-2015. *Morb. Mortal. Wkly. Rep. Surveill. Summ. Wash. DC* 2002
552 66, 1–12. <https://doi.org/10.15585/mmwr.ss6622a1>
- 553 Seinost, G., Dykhuizen, D.E., Dattwyler, R.J., Golde, W.T., Dunn, J.J., Wang, I.N., Wormser, G.P.,
554 Schriefer, M.E., Luft, B.J., 1999. Four clones of *Borrelia burgdorferi* sensu stricto cause invasive
555 infection in humans. *Infect. Immun.* 67, 3518–3524.
- 556 States, S.L., Brinkerhoff, R.J., Carpi, G., Steeves, T.K., Folsom-O’Keefe, C., DeVeaux, M., Diuk-Wasser,
557 M.A., 2014. Lyme disease risk not amplified in a species-poor vertebrate community: similar
558 *Borrelia burgdorferi* tick infection prevalence and OspC genotype frequencies. *Infect. Genet.*
559 *Evol. J. Mol. Epidemiol. Evol. Genet. Infect. Dis.* 27, 566–575.

560 <https://doi.org/10.1016/j.meegid.2014.04.014>
561 Tilly, K., Casjens, S., Stevenson, B., Bono, J.L., Samuels, D.S., Hogan, D., Rosa, P., 1997. The *Borrelia*
562 *burgdorferi* circular plasmid cp26: conservation of plasmid structure and targeted inactivation
563 of the *ospC* gene. *Mol. Microbiol.* 25, 361–373.
564 Vidakovic, B., 2011. *Statistics for Bioengineering Sciences: With MATLAB and WinBUGS Support.*
565 Springer Science & Business Media.
566 Wagemakers, A., Staarink, P.J., Sprong, H., Hovius, J.W.R., 2015. *Borrelia miyamotoi*: a widespread
567 tick-borne relapsing fever spirochete. *Trends Parasitol.* 31, 260–269.
568 <https://doi.org/10.1016/j.pt.2015.03.008>
569 Walter, K.S., Carpi, G., Evans, B.R., Caccone, A., Diuk-Wasser, M.A., 2016. Vectors as Epidemiological
570 Sentinels: Patterns of Within-Tick *Borrelia burgdorferi* Diversity. *PLOS Pathog.* 12, e1005759.
571 <https://doi.org/10.1371/journal.ppat.1005759>
572 Wang, G., Liveris, D., Mukherjee, P., Jungnick, S., Margos, G., Schwartz, I., 2014. Molecular Typing of
573 *Borrelia burgdorferi*. *Curr. Protoc. Microbiol.* 34, 12C.5.1-31.
574 <https://doi.org/10.1002/9780471729259.mc12c05s34>
575 Wang, I.-N., Dykhuizen, D.E., Qiu, W., Dunn, J.J., Bosler, E.M., Luft, B.J., 1999. Genetic Diversity of
576 *ospC* in a Local Population of *Borrelia burgdorferi sensu stricto*. *Genetics* 151, 15–30.
577 Wickham, H., 2009. *Ggplot2 elegant graphics for data analysis.* Springer, Dordrecht; New York.
578 Wormser, G.P., Brisson, D., Liveris, D., Hanincová, K., Sandigursky, S., Nowakowski, J., Nadelman, R.B.,
579 Ludin, S., Schwartz, I., 2008. *Borrelia burgdorferi* Genotype Predicts the Capacity for
580 Hematogenous Dissemination during Early Lyme Disease. *J. Infect. Dis.* 198, 1358–1364.
581 <https://doi.org/10.1086/592279>
582

583

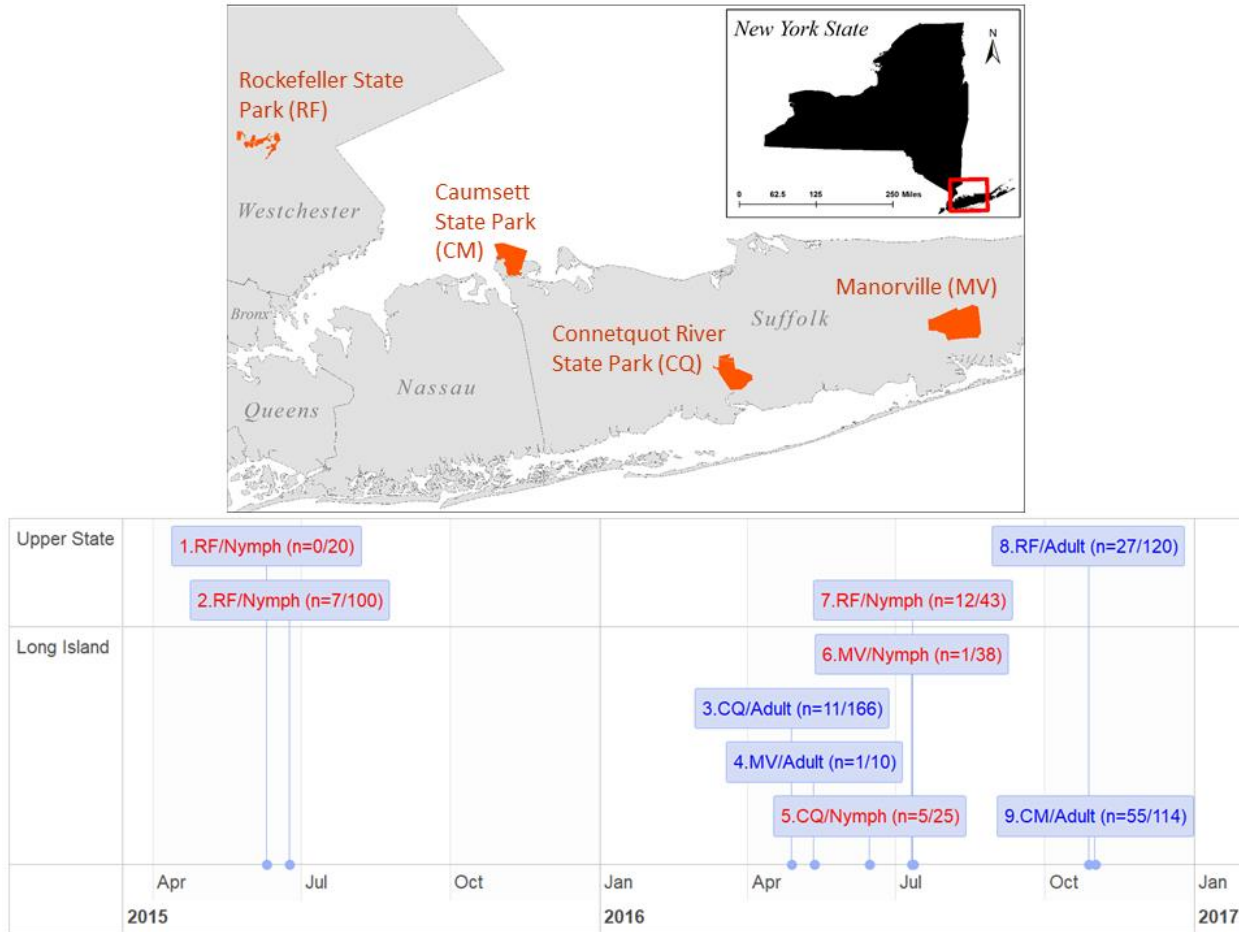
584 **Tables, Figure Legends, & Supporting Information**

585 **Table 1. Allele counts^a**

A	B	B3	C	C14	D	E	F	G	H	I	J	K	L	M	N	O	T	U	vsp	total
From Upper State, N=27 infected adult ticks (Pop 1)																				
2	4	0	7	0	1	6	0	7	2	3	0	3	4	2	5	0	5	4	2	57
From Upper State, N=19 infected nymphs (Pop 2)																				
3	3	0	1	1	1	4	1	1	3	0	0	2	1	2	2	2	2	0	3	32
From Long Island, N=67 infected adult ticks (Pop 3)																				
12	8	1	4	0	5	12	18	16	10	14	4	17	0	8	8	8	24	13	10	192
From Long Island, N=6 infected nymphs (Pop 4)																				
3	0	0	1	0	0	3	3	2	2	2	3	1	0	3	3	3	0	1	4	34
Sums																				
20	15	1	13	1	7	25	22	26	17	19	7	23	5	15	18	13	31	18	19	315

586 ^aSee Figure 5 for allele frequency distributions

587

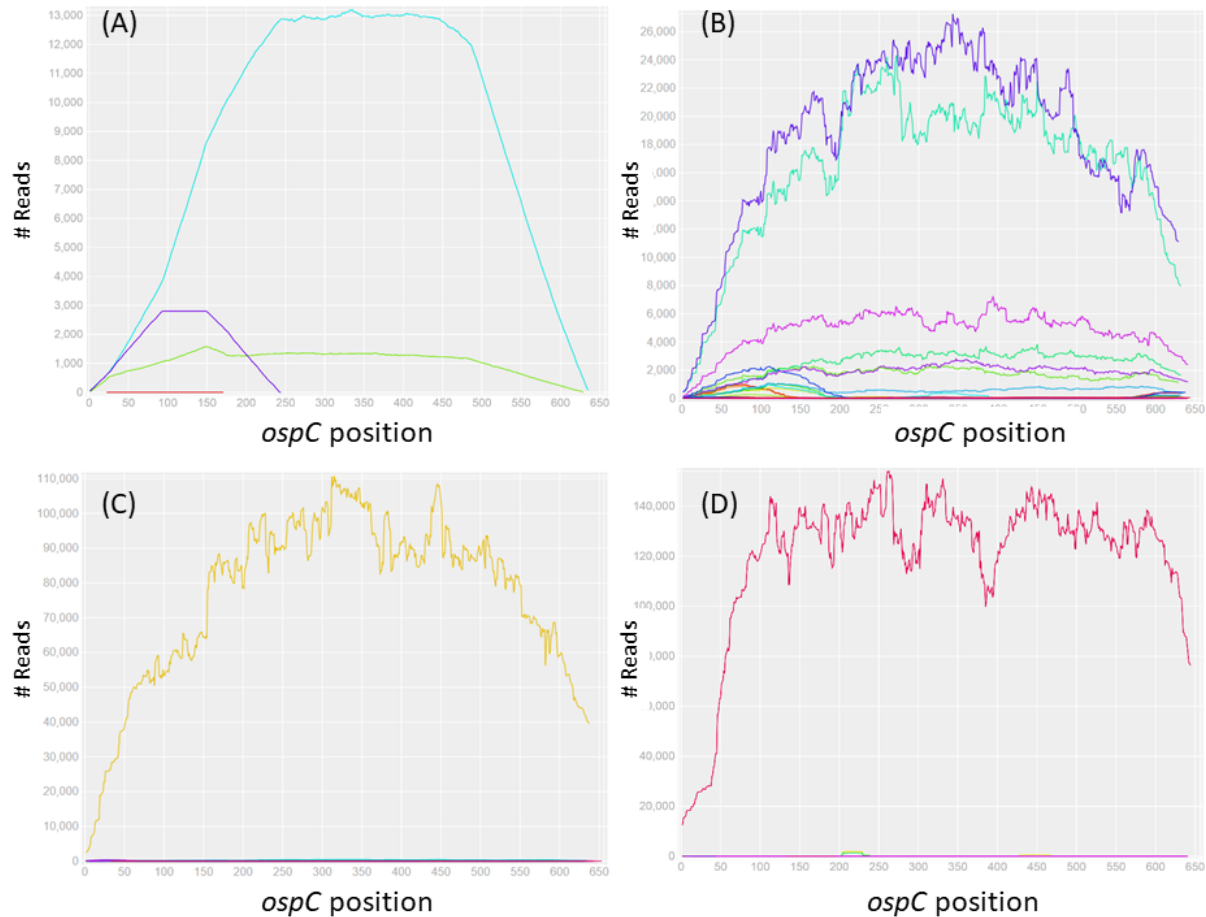


588

589 **Figure 1. Study sites and timeline**

590 Adult and nymphal *Ixodes scapularis* ticks were collected from four study sites in New York State,
 591 US (*top*) during their host-questing seasons in a period of 18 months (*bottom*). Nymphal samples
 592 are colored in red and adult samples in blue. Numbers in parenthesis indicate the number of ticks
 593 infected by Lyme disease spirochetes (numerator) and the total sample size (denominator).

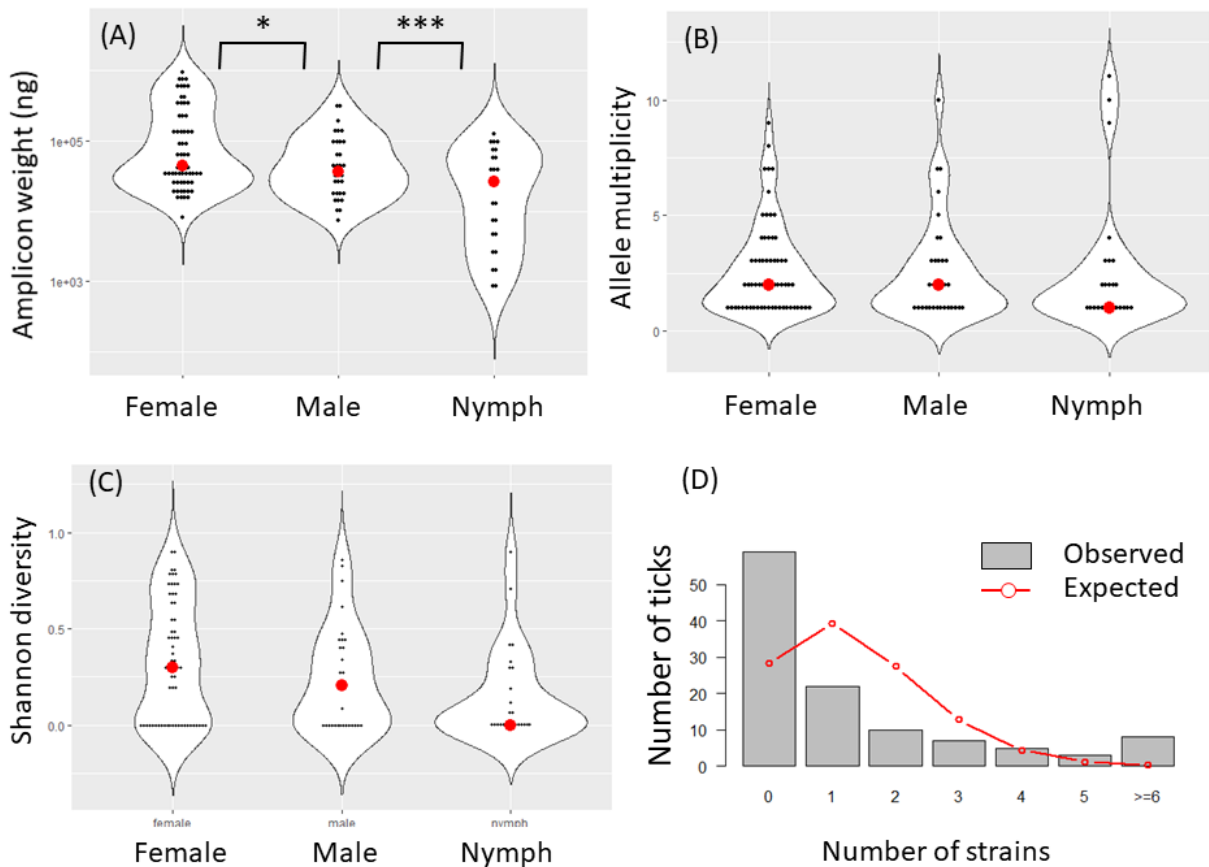
594



595

596 **Figure 2. Read depths of *ospC* alleles in simulated (A) and tick (B, C, D) samples**

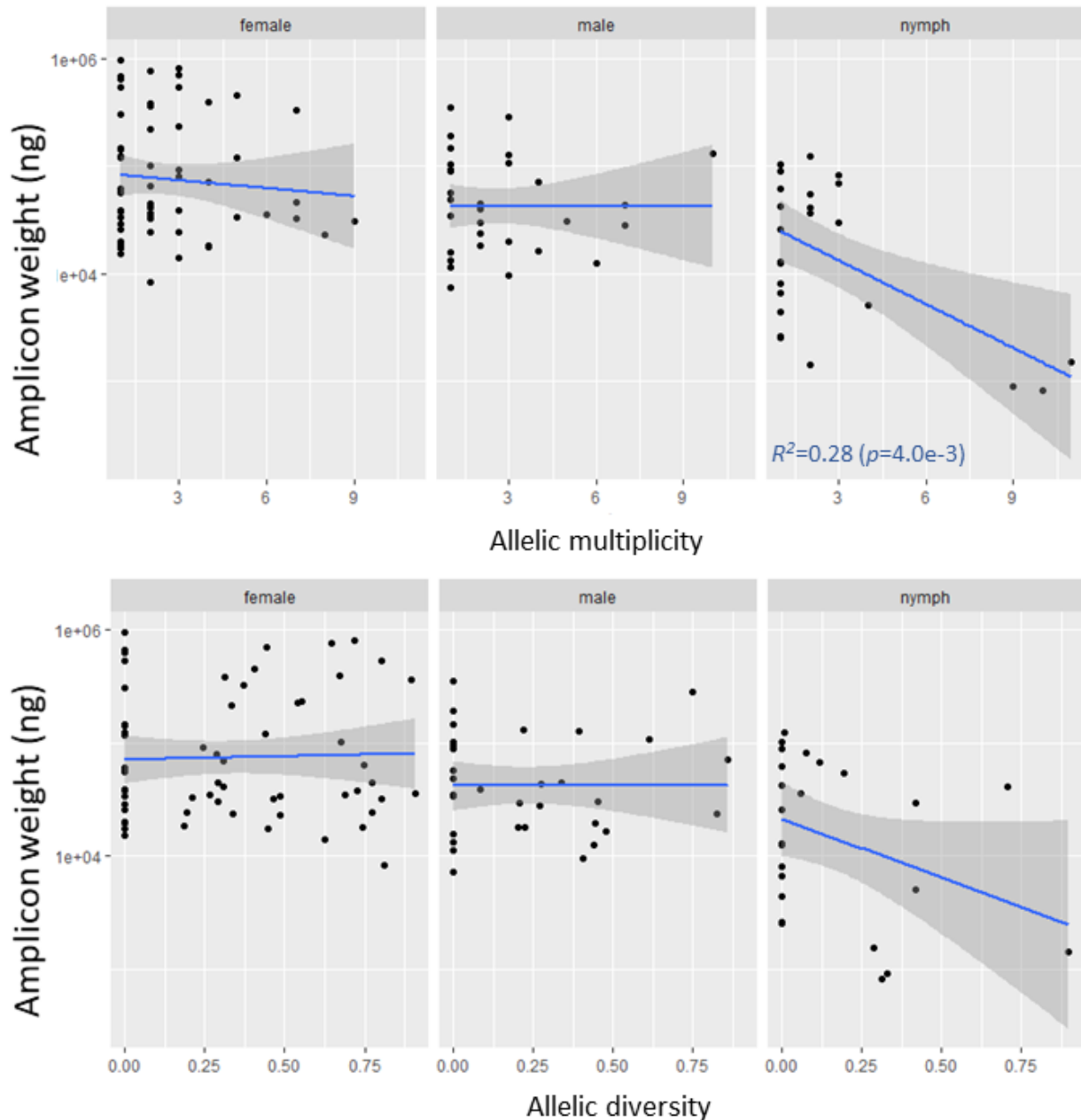
597 (A) Simulated reads are generated based on nucleotide sequences of two *ospC* alleles (J and C)
598 which are subsequently mixed in a 10:1 proportion. The reads are aligned to all 20 reference
599 sequences (Supplemental Material S2) and only the two input alleles show complete, full-length
600 coverages and approximately the same input proportion, validating the specificity and sensitivity
601 of the bioinformatics protocol for allele identification (a full test of specificity is shown in
602 Supplemental Material S4). (B) Seven *ospC* alleles (O, I, U, H, T, E, and K) are detected in an
603 adult tick (#M119, male, RF, Fall 2016). (C) The universal *ospC* primer set is able to amplify not
604 only the *ospC* locus in *Borreliella* species but also the *vsp* locus in *Borrelia miyamotoii* (see
605 alignment in Supporting Material S1). Here the *vsp* locus is detected in a nymph tick (#N030, RF,
606 Summer 2015). (D) A previously unknown *ospC* allele (“C14”, GenBank accession MH071431)
607 is detected in a nymph tick (N150, RF, Summer 2016), suggesting presence of a new *B. bissettiae*-
608 like species.



609

610 **Figure 3. Spirochete load & diversity**

611 (A) Spirochete loads, estimated with the weight of amplicons (y-axis, log₁₀ scale), are
612 significantly higher in female ticks than in males ticks, which in turn is higher than in nymphal
613 ticks. (B) There is no significance differences among the three life stages in strain diversity as
614 measured by the number of distinct strains within a tick (“multiplicity”). (C) Shannon diversity,
615 which takes allele frequencies into account (see Material & Methods), is also not significantly
616 different among the tick stages. These results support the notion that strain diversity in individual
617 ticks is contributed more by a mixed inoculum in hosts than by the number of blood meals (Walter
618 et al., 2016). (D) Observed counts of infected and uninfected adult ticks (N=144 from Sample #9,
619 Figure 1). Expected counts are based on a Poisson model assuming that strains infect ticks
620 independently. The observed distribution shows an over-abundance of uninfected ticks and ticks
621 infected by five or more strains, while an under-abundance of ticks infected by 1-3 strains,
622 suggesting reservoir hosts tend to be either uninfected or repeatedly infected.

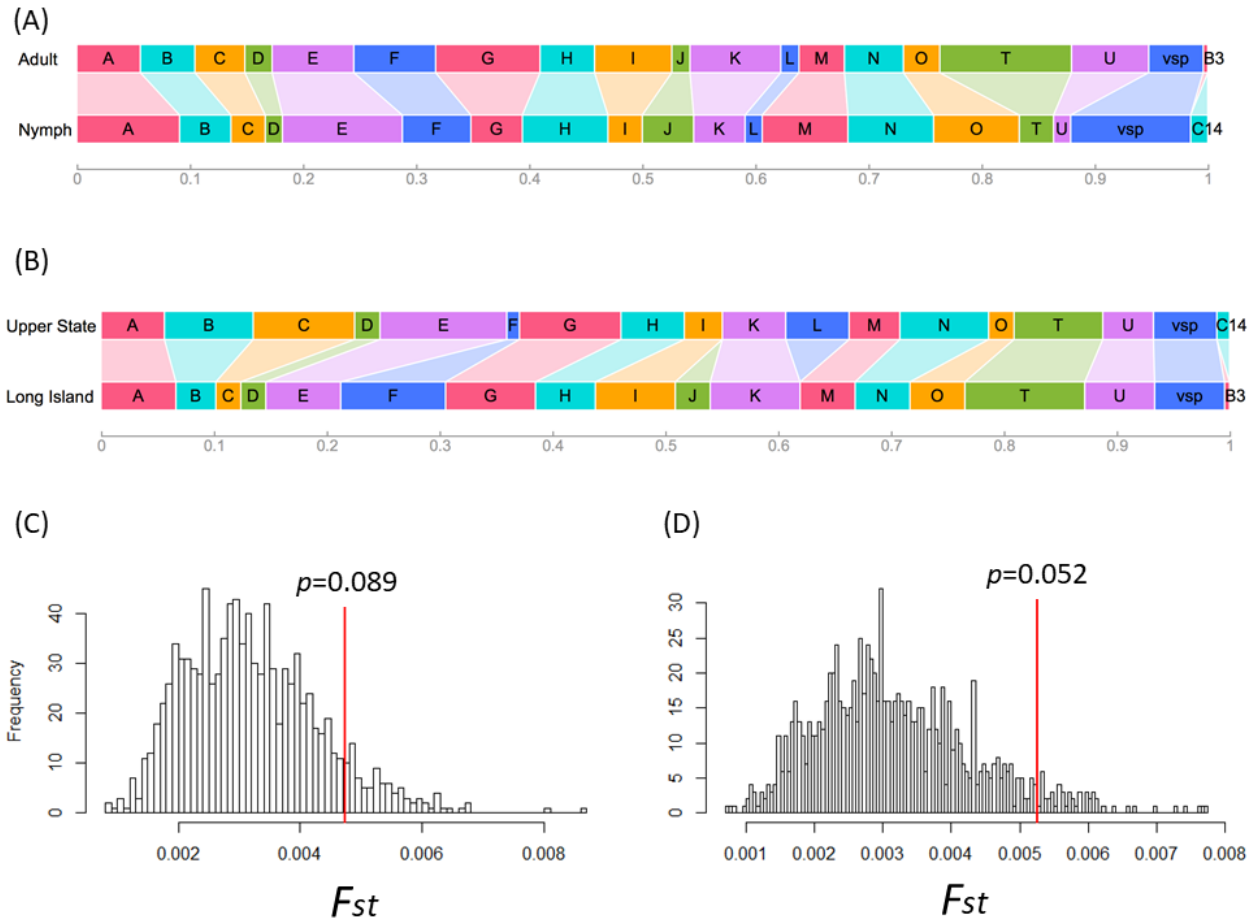


623

624 **Figure 4. Negative interactions among co-infecting strains**

625 (A) Spirochete load is either flat or decreasing with increasing strain multiplicity, supporting
626 inhibitory interactions among co-infecting strains (Durand et al., 2017; Walter et al., 2016). (B)

627 The pattern of inhibitory interactions holds when strain diversity is measured by Shannon
628 diversity.



629

630 **Figure 5. Geographic and life-stage differences in pathogen strain composition**

631 (A) Strain composition (width of each colored rectangle representing frequency of an allele in a
 632 population sample) between those infecting adult ticks (Pop1+Pop3, see Table 1) and those
 633 infecting nymph ticks (Pop2 + Pop4). (B) Strain compositions in two regional populations (Upper
 634 State, Pop1 + Pop2; Long Island, Pop3 + Pop4;). (C) There is no significant genetic difference in
 635 strain composition between those infecting adult and those infecting nymph ticks (p value obtained
 636 by resampling 999 times; see Material & Methods). (D) Two regional populations show non-
 637 significant albeit stronger genetic differentiation.

638

639

640 **Supplemental Material**

641 Text S1. Design of universal *ospC* primers for full-length amplification

642 Text S2. Nucleotide sequences of 20 *ospC* alleles used as references for strain identification

643 Text S3. Bioinformatics protocols

644 Figure S4. Specificity of allele identification

645 Figure S5. Strain distribution within infected ticks

646

647